

RESEARCH PAPER



miR-29a-3p mitigates the development of osteosarcoma through modulating IGF1 mediated PI3k/Akt/FOXO3 pathway by activating autophagy

Song Qi^{a*}, Li Xu^{a*}, Yongyuan Han^b, Hongkun Chen^c, and Anyuan Cheng^a

^aDepartment of Trauma Surgery, Wuhan No 1 Hospital, Wuhan, Hubei, China; ^bOrthopedics Department I, Zaozhuang Chinese Medicine Hospital, Zaozhuang, Shandong, China; ^cPediatric Surgery, Zaozhuang Municipal Hospital, Zaozhuang, Shandong, China

ABSTRACT

Osteosarcoma (OS), occurring in mesenchymal tissues and with a high degree of malignancy, is most common in children and adolescents. At present, we intend to figure out the expression and functions of miR-29a-3p in OS development. Reverse transcription-polymerase chain reaction (RT-PCR) was adopted to monitor the expression of miR-29a-3p and IGF1 in OS tissues and adjacent non-tumor tissues. Then, the 3- (4,5)-dimethylthiazolium (-z-y1)-3,5-di- phenyltetrazoliumromide (MTT) assay, colony formation experiment, western blot and Transwell assay were conducted to validate OS cell proliferation, colony formation ability, apoptosis, migration and invasion. Next, the association between miR-29a-3p and IGF1 was corroborated by the dual-luciferase reporter assay and the Pearson correlation analysis. Finally, WB was implemented to test the levels of autophagy-related proteins LC3-I/LC3-II, Beclin-1, p62, and the IGF-1 R/PI3k/Akt/FOXO3 axis in OS cells. As a result, miR-29a-3p was down-regulated in OS tissues (versus adjacent non-tumor tissues) and OS cell lines. Overexpressing miR-29a-3p aggravated apoptosis, dampened cell proliferation, colony formation, migration and invasion, and promoted autophagy of OS cells. IGF1 was identified as a target of miR-29a-3p. IGF1 induced oncogenic effects in OS by activating IGF-1 R/ PI3k/Akt pathway, and it dampened the tumor-suppressive effect of miR-29a-3p on OS. Taken together, miR-29a-3p repressed the OS involvement through inducing autophagy and inhibiting IGF1 mediated PI3k/Akt/FOXO3 pathway.

ARTICLE HISTORY

Received 5 January 2021
Revised 20 March 2022
Accepted 11 May 2022

KEYWORDS

miR-29a-3p; IGF1;
osteosarcoma; progression;
signaling pathway



1 Introduction

Osteosarcoma (OS) is a primary malignancy that originates in the metaphysis of the long bones, principally affecting children, adolescents and young people. The treatment of OS is mainly surgical resection in conjunction with systemic adjuvant chemotherapy, and the 5-year survival rate of patients after treatment is about 60–70% [1]. Disappointingly, decades of research have failed to significantly improve the overall survival rate of OS patients, especially those with lung or bone metastasis, which is below 30% [2]. There is therefore an urgent need to address novel molecular markers and to work toward their application in clinical strategies against OS.

Autophagy is a process of cell catabolism that maintains the homeostasis of cells under stress. Dysregulation of autophagy leads to the emergence of various diseases, of which neurodegenerative

diseases, inflammatory disorders and cancer are examples [3]. Therefore, the autophagy inducers can be used to treat certain malignant tumors [4]. More importantly, studies have confirmed that activating autophagy suppresses OS and accelerates tumor cell apoptosis [5]. For example, miR-193b induces autophagy and apoptosis of OS, thereby increasing its chemosensitivity [6].

MicroRNAs (miRNAs) are small noncoding RNAs that control the expression of downstream target genes by degrading mRNAs or inhibiting their translation post-transcriptionally. It is worth noting that miRNAs exert carcinogenic or anti-tumor effects in diversified cancers [7]. As an example, miR-150-5p enhances cell proliferation of colon cancer via targeting the tumor suppressor gene TP53 [8]. In contrast, miR-150-5p abates the metastasis and recurrence in non-small cell lung cancer (NSCLC) by targeting high

CONTACT Anyuan Cheng  whucay@whu.edu.cn  Department of Trauma Surgery, Wuhan No 1 Hospital, 215 Zhongshan Avenue, Wuhan, 430022, Hubei, China.

#Contributed equally

mobility group AT-hook 2 and β -Catenin [9]. In addition, it is suggested that miRNAs also play a major part in OS. For instance, miR-342-5p is lowly expressed in OS tissues and cell lines. miR-342-5p overexpression substantially restrains OS cell viability and invasion, while augmenting OS cell apoptosis [10]. miR-142-3p and miR-129-5p are down-regulated in OS tissues and cell lines, where they choke OS cell growth and induce OS cell apoptosis by targeting HMGB1 [11]. Besides, miR-506 [12] and miR-188-5p [13] also act as tumor suppresser genes that curb the malignant advancement of OS. As a miRNA, miR-29a-3p bridles colorectal cancer [14] and hepatocellular carcinoma [15]. Nonetheless, the contribution of miR-29a-3p in OS is still difficult to define.

Insulin-Like Growth factor-1 (IGF1) consists of 70 amino acids and weighs 7.6 KDa. There is evidence that IGF1 exerts a carcinogenic function in tumors by amplifying tumor proliferation and inhibiting apoptosis. For instance, Su et al. found that IGF1 up-regulates matrix metalloproteinase-11 and enhances cell proliferation and invasion in gastric cancer by stimulating the JAK/STAT3 axis [16]. Also, IGF1 is found to be abnormally expressed in OS and is a potential target for OS treatment [17]. Moreover, the phosphoinositide 3-kinase/serine/threonine kinase (PI3k/Akt) pathway controls cell growth, migration, proliferation, and metabolism in mammalian cells and is a commonly deregulated pathway in cancer. Previous research revealed that dampening the SCL/TAL1 interrupting locus down-regulates the IGF1/PI3k/Akt axis, thereby delaying gastric cancer progression [18]. Moreover, the PI3k/Akt activation in OS accelerates tumor metastasis [19]. The Forkhead Box Transcription Factors3 (FOXO3) is considered to be a tumor-related transcription factor that modulates cell cycle arrest and apoptosis. Brunet et al. showed that the activation of Akt degrades FOXO3, thus hindering apoptosis, which makes FOXO3 a possible therapeutic target for cancer [20,21]. Interestingly, Zhou et al. found that miR-135a promotes NSCLC apoptosis through the IGF-1/PI3k/Akt signal and inhibits cell proliferation, migration, invasion and tumor angiogenesis [22]. Hence, we speculate the regulation of miR-29a-3p on the IGF-1/PI3k/Akt pathway also influences OS evolvement.

Presently, we aim to make clear the exact mechanism of miR-29a-3p in the development of OS, possibly through regulating the IGF-1/PI3k/Akt pathway. It was discovered that miR-29a-3p was down-regulated in OS, and overexpressing miR-29a-3p abated OS development by activating autophagy and inhibiting the IGF1/PI3k/Akt axis, which may be the breakthrough of the new treatment for OS.

2 Materials and methods

2.1 Clinical samples

The OS tissues and adjacent non-tumor tissues (at least 1 cm from the OS boundary) were collected from OS patients who received surgery in Zaozhuang Municipal Hospital. The researched subjects were not treated with radiotherapy or chemotherapy before the operation, and the clinical specimens were diagnosed by the pathology department of Zaozhuang Municipal Hospital. After the samples were collected, they were placed in -80°C liquid nitrogen and stored frozen until the experiment was performed. All patients signed an informed agreement. This research was granted and supported by the ethics committee of Wuhan No 1 Hospital.

2.2 Cell culture and transfection

Human OS cell lines 143B, MG-63, HOS, SJSA-1 and normal osteoblasts hFOB 1.19 were bought from American Type Culture Collection (ATCC, Rockville, MD, USA). The above cells were inoculated in the high glucose DMEM medium comprising 10% fetal bovine serum and 1% streptomycin (Thermo Fisher HyClone, Utah, USA) at 1×10^5 cells/mL and then were routinely cultured at 37°C with 5% CO_2 under completely saturated humidity for further experiments. Cells were transfected using Lipofectamine 3000 as per the manufacturer's directions (ThermoFisherScience, Waltham, MA, USA). Briefly, MG-63 and HOS cells in the logarithmic growth phase were taken and the cell density was adjusted to achieve 80%-90% fusion. Next, the cells were inoculated into 12-well plates. Afterward, the DMEM medium was used for culture, and the primary culture medium was discarded on the next day

for transfection. Subsequently, Agomir-miR-29a-3p (40 nM) and agomir-NC (40 nM) were transfected using Lipofectamine 2000 (Invitrogen, Carlsbad, CA, USA) with the aid of the manufacturer's directions. agomir-miR-29a-3p and agomir-NC were synthesized by Ribobio Biotech Co., Ltd. (Guangzhou, China). Twenty-four hours after the transfection, the culture medium was substituted with a fresh complete one, and reverse transcription-polymerase chain reaction (RT-PCR) was performed to confirm the transfection efficiency.

2.3 RT-PCR

MG-63 and HOS cells were taken, and the total RNA was obtained utilizing the TRIzol method (Invitrogen, Carlsbad, CA, USA). In contrast, miRNAs were isolated with the use of the mirPremier[®] microRNA Isolation Kit (Sigma, St. Louis, MO, USA). The One Step PrimeScript miRNA cDNA synthesis kit (Bao Biological Engineering Co., Ltd., Dalian, China) and the PrimeScript RT kit (Madison, WI, USA) were adopted to transcribe miR-29a-3p and IGF1 into cDNA, respectively. We then conducted RT-PCR by employing SYBR[®]Premix-Ex-Taq[™] (Takara, TX, USA) and the ABI7300 system. GAPDH served as the housekeeping gene for IGF1, while U6 served as that for miR-29a-3p. The primer sequences included: miR-29a-3p, F:5'-GATGTGCCTTGCTGGGAAA-3'; R: 5'-ACCGGAGACATCTACGTTGCT-3'; IGF1, F:5'-TGTGCTTCTTGACGACTTGC-3'; R: 5'-CTGAATCTTGGCTGCTGGA-3'; GAPDH, F:5'-TGGTTGAGCACAGGGTACTT-3'; R:5'-CCAAGGAGTAAGACCCCTGG-3'. U6: F:5'-CTCGCTTCGGCAGCAGCACATATA-3'; R:5'-AAATATGGAACGCTTCACGA-3'. The relative expression was calculated based on the $2^{-\Delta\Delta CT}$ value of each gene, and all experiments were made three times.

2.4 3-(4,5)-dimethylthiazolide (-z-y1)-3,5-diphenyltetrazoliumromide (MTT) assay

MG-63 and HOS cells were harvested to make cell suspensions (1×10^4 /mL) after the trypsinization. Then, the suspensions were inoculated in 96-well

plates (200 μ L/well) and cultured at 37°C with 5% CO₂ and saturated humidity for 24, 48, 72, 96 and hours, respectively. Afterward, the primary medium was substituted with a fresh one, with 20 μ L MTT solution (5 g/L) supplemented and maintained for another 4 hours. Subsequently, the medium was removed, and each well was supplemented with 150 μ L DMSO, which was shaken in the dark for 10 min to dissolve the crystals. The absorbance of each well was determined at 490 nm with a microplate reader (Bio-Rad Laboratories, Hercules, CA, USA), and the experiment was repeated three times.

2.5 Colony formation experiment

The transfected MG-63 and HOS cells were seeded in 6-well plates at 1000 cells/well and incubated at 37°C with 5% CO₂ for two weeks. Colony formation analysis was carried out following the method of Wang Y et al. [23]. Then, the cells were carefully flushed three times with PBS, immobilized with methanol for 20 min and dyed with crystal violet for 1 min. After that, the staining solution was washed away with running water. At last, the number of colonies per well was calculated under an optical microscope (Olympus, Tokyo, Japan).

2.6 Flow cytometry

The AnnexinV-FITC double staining method was implemented to test apoptosis. Following transfection, MG-63 and HOS cells were trypsinized, inoculated in 6-well plates at 2×10^6 /well, and cultured for another 24 hours, with the supernatant discarded. The above-treated cells were rinsed with PBS and then fastened in 70% ethanol. Afterward, the fixed cells were rinsed with PBS again, supplemented with 5 μ L AnnexinV-FITC and 5 μ L PI, mixed well, and incubated at room temperature (RT) for 15 min. A flow cytometer (Beckman Coulter, Fullerton, CA, USA) was adopted to measure the apoptosis rate within 1 hour. Apoptosis rate = number of apoptotic cells/(number of apoptotic cells + number of normal cells) \times 100%.

2.7 Transwell assay

Transwell assay was implemented to monitor cell migration and invasion. MG-63 and HOS cells were inoculated in the upper transwell chamber at 5×10^4 /well, and 600 μ L of the culture medium supplemented with 10% FBS was added to the lower chamber and cultured at 37°C. After 12 hours, the cells in the upper chamber were wiped off, secured with 4% paraformaldehyde, dyed with 0.1% crystal violet, dried, photographed, and calculated. For the cell invasion experiment, the upper chamber was pre-coated with matrigel (Biosciences, Lincoln, NE) and seeded with cells, and the other procedures were the same as for the migration assay.

2.8 Western blot (WB)

The transfected MG-63 and HOS cells were collected, lysed with RIPA lysate (Beyotime Biotechnology, Shanghai, China) to extract the protein. Then, the BCA method (Pierce, Appleton, WI, USA) was applied to evaluate the protein content. Afterward, the equivalent quantity of protein was loaded on 12% SDS-PAGE and transferred to the PVDF membranes, which were then maintained with the primary Anti-LC3I/II antibody (ab128025, 1:1000, Abcam, USA), Anti-Beclin1 antibody (ab207612, 1:1000, Abcam, USA), Anti-p62 antibody (ab91526, 1:1000, Abcam, USA), Anti-IGF1 antibody (ab106836, 1:1000, Abcam, USA), Anti-PI3k antibody (Phosphatase) (SRP5280, 1:1000, sigma, USA), Anti-PI3k antibody (ab140307, 1:1000, Abcam, USA), Anti-Akt (phospho T308) antibody (ab38449, 1:1000, Abcam, USA), Anti-Akt antibody (SAB4500797, 1:1000, sigma, USA), Anti-FOXO3 antibody (SAB2107951, 1:1000, sigma, USA), Anti-Bax antibody (ab32503, 1:1000, USA), Anti-Bcl-2 antibody (ab32124, 1:1000, USA), Anti-Bad antibody (ab32445, 1:1000, USA), Anti-E-cadherin antibody (ab40772, 1:1000, USA), Anti-N-cadherin antibody (ab76011, 1:1000, USA), Anti-Vimentin antibody (ab92547, 1:1000, USA), Anti-Snail antibody (ab216347, 1:1000, USA), Anti-IGF-1 R antibody (ab182408, 1:1000, USA); Anti-IGF-1 R (phospho Y1161) antibody (ab39398, 1:1000, USA) and Anti-GAPDH

antibody (ab181602, 1:1000, Abcam, USA) at 4°C overnight. After being flushed with PBST, the membranes were rinsed with the HRP-tagged specific secondary antibody Goat Anti-Rabbit IgG (ab150077, 1:3000, Abcam, USA) at RT for 2 hours and then rinsed 3 times with PBST. GAPDH served as the internal reference. The Image Lab system (Bio-Rad, Shanghai, China) was employed to quantify the band intensity.

2.9 Tumor formation experiment in nude mice

Female BALB/c nude mice (6–8 weeks old) were bought from the Animal Experiment Center of Huazhong University of Science and Technology and were raised in an SPF-free environment. MG-63 cells were transfected with agomir-miR-29a-3p (40 nM) and agomir-NC (40 nM) for 24 hours, and then made into single-cell suspensions. Then, the cells were adjusted to 2×10^6 /mL and subcutaneously injected into each nude mouse, which was fed under SPF. The mice's diet, activity and general condition were closely monitored. The mice's tumor volumes were gauged from the 12th day after the subcutaneous injection and thereafter assayed every four days. Tumor volume = length \times width² \times 0.5. The mice were sacrificed six weeks later, and the tumor was carefully peeled off, weighed, and subjected to WB and IHC.

2.10 Dual-luciferase reporter assay

The targeting association between miR-29a-3p and the 3'-untranslated region (3'-UTR) of IGF1 was validated by the dual-luciferase reporter gene assay. TargetScan (<http://www.targetscan.org/>) predicted that IGF1 was an essential target for miR-29a-3p. The WT 3'-UTR fragment of the wild-type (WT) IGF1 sequence was amplified and inserted into the pmirGLO dual-luciferase miRNA target expression vector (Promega Corp., Madison, WI, USA) to build the reporter vector pmirGLO-IGF1-WT. The GeneArt™ Site-Directed Mutagenesis PLUS System (cat. no. A14604; Thermo Fisher Scientific, Inc.) was adopted to mutate the putative binding site of the miR-29a-3p family in IGF1 3'-UTR. In parallel, the mutant (MUT) IGF1 3'-UTR was inserted into the pmirGLO vector to form the reporter vector

pmirGLO-IGF1 -MUT. The corresponding reporter vectors (80 ng/ml) and miR-29a-3p agomir (40 nmol/L) or agomir-NC (40 nmol/L) were co-transfected into MG-63 and HOS cells and then incubated for 48 hours. After that, the experiment was done by observing the guidelines of dual-luciferase detection (Promega, Beijing, China). The relative fluorescence intensity of different treatment groups was established based on the ratio of firefly fluorescence intensity/renilla fluorescence intensity gauged by the microplate reader.

2.11 Statistical analysis

The GraphPad Prism 6 software (GraphPad Software, Inc., city, state) was applied for analysis. The measurement data were denoted by mean \pm standard deviation ($\bar{x} \pm s$). One-way ANOVA was employed for multivariate comparison, and the student's *t* test was utilized to compare the two groups. The correlation between miR-29a-3p and IGF1 was determined by the Pearson correlation test. $P < 0.05$ was deemed statistically significant.

3 Results

3.1 miR-29a-3p was down-regulated in OS tissues and cells

Firstly, the miR-29a-3p profile was verified by RT-PCR, confirming that miR-29a-3p's expression was

downregulated in OS tissues compared with that in the adjacent non-tumor tissues ($P < 0.05$, Figure 1(a)) and lower in OS cell lines versus in normal human osteoblast hFOB 1.19 ($P < 0.05$, Figure 1(b)). Additionally, by analyzing the association between the miR-29a-3p level and clinical sample characteristics, we discovered that the lower miR-29a-3p expression indicated later clinical stages of OS patients and more significant distant metastasis ($P < 0.05$, Table 1). The above conclusions illustrated miR-29a-3p was linked to a better prognosis of OS patients.

3.2 miR-29a-3p hindered OS cell proliferation, colony formation, migration and invasion, and facilitated apoptosis

To assay the impact of miR-29a-3p on OS cells, we transfected miR-29a-3p agomir and negative control agomir-NC in MG-63 and HOS cells and checked the miR-29a-3p profile in cells at days 1, 3, 7 and 14 after transfection. The outcomes displayed that miR-29a-3p was up-regulated in MG-63 and HOS cells transfected with miR-29a-3p agomir versus the NC group, with the most pronounced up-regulation at day 1 and day 3 (Figure 2(a)). Next, OS cell proliferation, colony formation, migration, invasion, and apoptosis were detected with different methods. The data substantiated that up-regulating miR-29a-3p attenuated OS cells' proliferation and colony formation (Figure 2

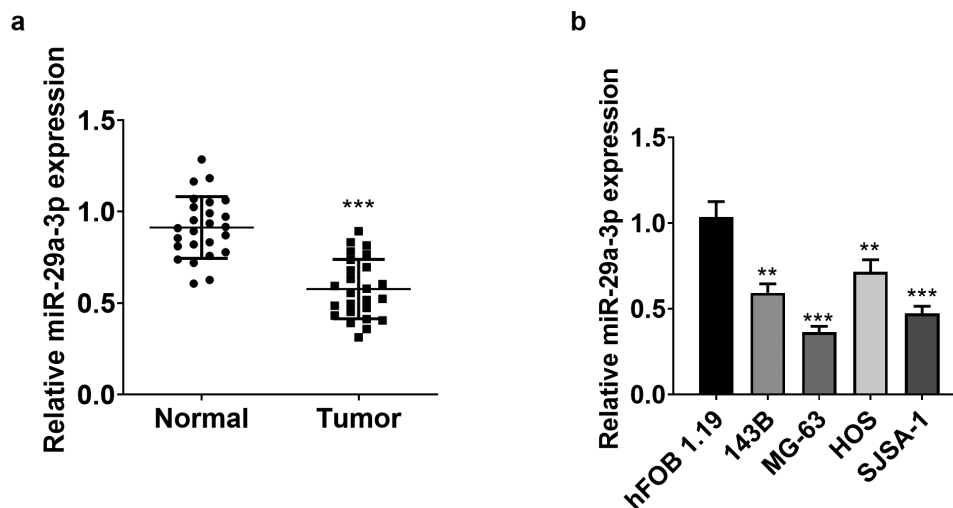


Figure 1. miR-29a-3p was down-regulated in OS tissues and cells. A-B. RT-PCR gauged the level of miR-29a-3p in OS tissues and the adjacent non-tumor tissues (A) and in human OS cell lines 143B, MG-63, HOS, SJS-A-1 and normal human osteoblast hFOB 1.19 (B). **, *** represents $P < 0.01$ and $P < 0.001$ vs. Normal group or hFOB 1.19 group.

Table 1. Association between clinicopathological features and the miR-29a-3p expression in OS tissues (n = 25).

Variable	miR-29a-3p Expression		P-value
	Low (n = 16)	High (n = 9)	
Age	10	6	0.835
≤20	6	3	
>20			
Gender	7	5	0.571
Female	9	4	
male			
Tumor size	8	3	0.420
≤8 cm	8	6	
>8 cm			
TNM	12	2	0.011*
I-II	4	7	
III-IV			
Distance metastasis	3	6	0.006*
Yes	13	3	
No			

* $P < 0.05$, the difference was significant

(b-d)). Additionally, flow cytometry data exhibited that enhancing the miR-29a-3p level intensified OS cell apoptosis (Figure 2(e)). As revealed by the WB data, up-regulating miR-29a-3p caused facilitation in the expression of the pro-apoptotic proteins Bax and Bad and attenuation in the profiles of the apoptosis-inhibitory protein Bcl-2 in MG-63 and HOS cells versus the NC group (Figure 2(f)). Moreover, the transwell result indicated that OS cells' migration and invasion were distinctly choked following miR-29a-3p overexpression (Figure 2(f)). In addition, WB outcomes displayed that up-regulating miR-29a-3p enhanced the E-cadherin expression and restrained the levels of N-cadherin, Vimentin, and Snail in MG-63 and HOS cells in comparison to the NC group (Figure 2(g)). Taken together, miR-29a-3p repressed OS development.

3.3 miR-29a-3p induced autophagy and inactivated the PI3k/Akt/FOXO3 axis

We performed WB to compare the levels of autophagy-related proteins LC3II/LC3I, Beclin1 and p62, and the IGF-1 R and PI3k/Akt/FOXO3 pathways to probe the mechanism underlying the inhibition of OS progression by miR-29a-3p. The results manifested the miR-29a-3p mimics' transfection facilitated the expression of LC3II/LC3I and Beclin1 and attenuated p62 (Figure 3(a)). Furthermore, forced miR-29a-3p expression abated p-IGF-1 R, p-PI3k and p-Akt and enhanced the FOXO3 level ($P < 0.05$, Figure 3(b)). Thus, miR-29a-3p facilitated

the autophagy of OS cells by attenuating the PI3k/Akt/FOXO3 pathway.

3.4 miR-29a-3p abated OS growth *in vivo* and induced autophagy

Further, we characterized the role of miR-29a-3p in OS *in vivo*. Briefly, MG-63 cells transfected with agomir-miR-29a-3p were subcutaneously administered to nude mice, and tumor volume and weight were observed and measured. The results illustrated that the tumor volume and weight in the miR-29a-3p group were lower versus the NC group ($P < 0.05$, Figure 4(a-c)). Next, we performed IHC and discovered that tumor tissues with up-regulated miR-29a-3p had lower expression of Ki67 (Figure 4(d-e)), p-IGF-1 R (Figure 4(f)), p-PI3K (Figure 4(g)), and p-AKT (Figure 4(h)) versus the NC group. Then, the expression of autophagy-related proteins and p-PI3k and p-Akt were compared by WB. As a result, the transfection of agomir-miR-29a-3p strengthened LC3II/LC3I and Beclin1 levels *in vivo* and lowered p62 expression ($P < 0.05$, Figure 4(i)). Besides, miR-29a-3p abated p-IGF-1 R, p-PI3k and p-Akt while up-regulated FOXO3 as indicated by western blot result ($P < 0.05$, Figure 4(j)). At last, we gauged the miR-29a-3p profile in tumor tissues using RT-PCR, which uncovered that miR-29a-3p was notably up-regulated in the miR-29a-3p group versus the NC group ($P < 0.05$, Figure 4(k)). These conclusions confirmed that miR-29a-3p dampened OS growth, induced autophagy, inactivated the PI3k/Akt pathway, and up-regulated FOXO3 *in vivo*.

3.5 miR-29a-3p targeted the 3'UTR of IGF1

By querying the Starbase (<http://starbase.sysu.edu.cn/>), we corroborated that IGF1 was a vital downstream target of miR-29a-3p (Figure 5(a)). Then, the correlation between the two was determined by the dual-luciferase reporter assay. It turned out that the transfection of agomir-miR-29a-3p notably inhibited IGF1-WT, while it had little impact on IGF1-MUT ($P < 0.05$, Figure 5(b-c)). Next, Pearson correlation analysis affirmed that miR-29a-3p was reversely related to IGF1 ($R^2 = 0.425$, Figure 5(d)). Moreover, the IGF1 profile in OS

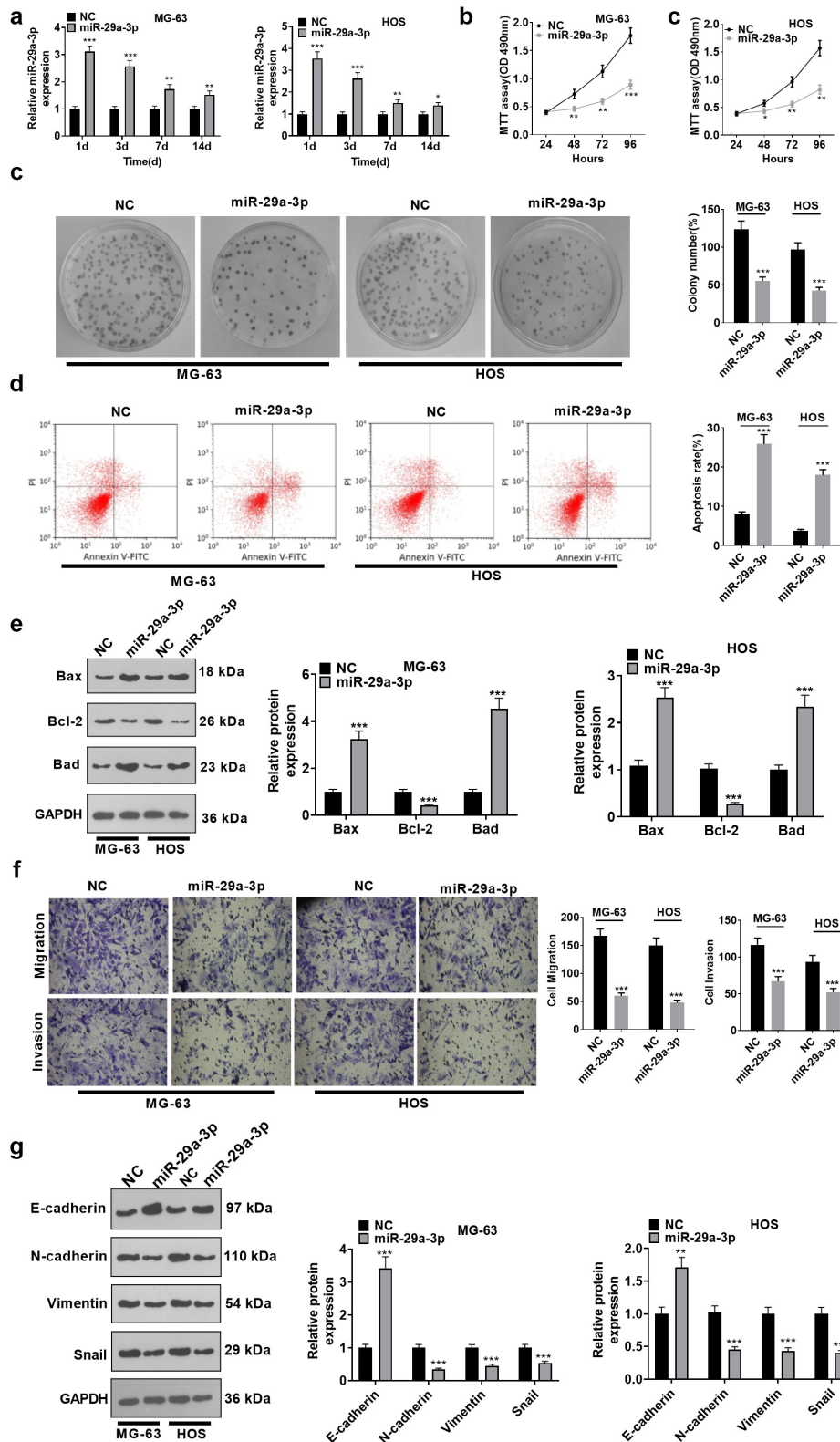


Figure 2. miR-29a-3p attenuated OS proliferation, colony formation, migration and invasion, and promoted apoptosis. The miR-29a-3p agomir and agomir-NC were transfected in MG-63 and HOS cells and cultured for 1–14 days. A: The miR-29a-3p profile in MG-63 and HOS cells was gauged using RT-PCR at days 1, 3, 7, and 14 after transfection with miR-29a-3p agomir and negative control. B–C: MTT was conducted to test cell proliferation, * $P < 0.05$; ** $P < 0.01$; *** $P < 0.001$ (Vs.NC group). D: The number of cell colonies formed was assessed using the colony formation experiment at day 14 of transfection with miR-29a-3p agomir and agomir-NC. E: Flow cytometry was carried out to validate apoptosis. F: WB assayed the levels of Bax, Bcl-2 and Bad in MG-63 and HOS cells. F: Cell migration and invasion were compared by Transwell assay. G: WB was applied to test the profiles of E-cadherin, N-cadherin, Vimentin, and Snail in MG-63 and HOS cells. Data were expressed as mean \pm SD. N = 3. * $P < 0.05$; ** $P < 0.01$; *** $P < 0.001$ vs.NC group.

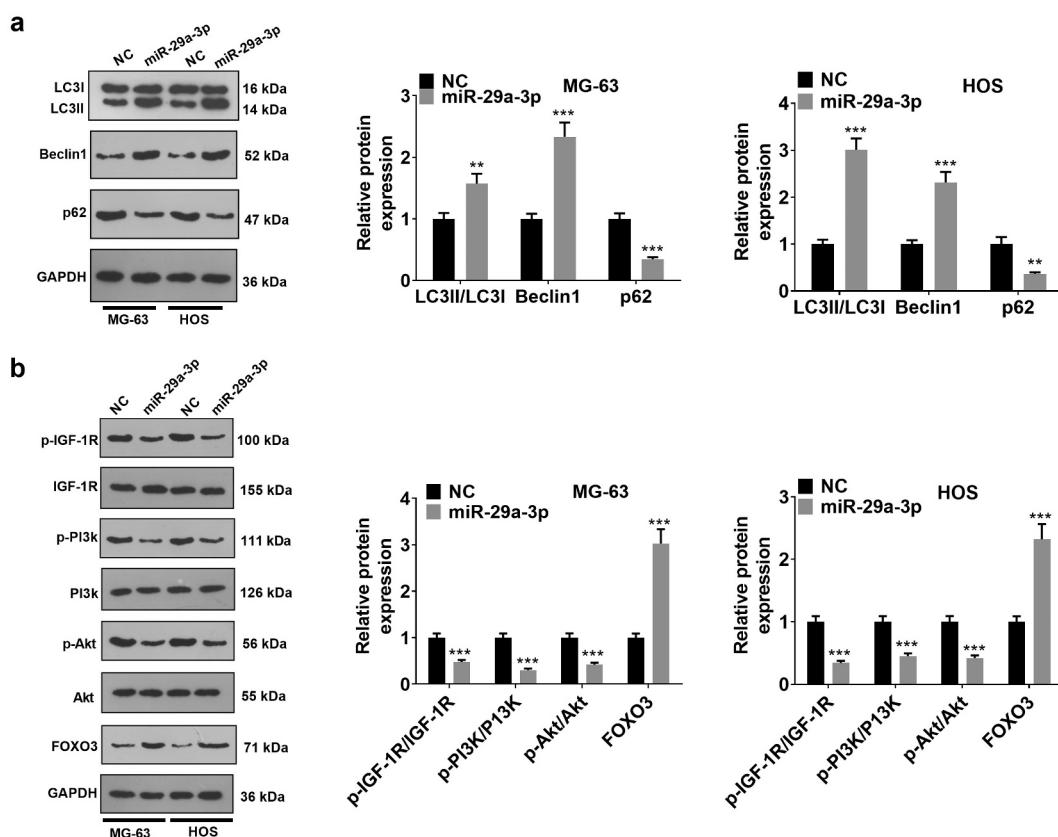


Figure 3. miR-29a-3p induced autophagy and choked the PI3k/Akt/FOXO3 pathway. miR-29a-3p agomir and agomir-NC were transfected into MG-63 and HOS cell lines. A-B: WB verified the LC3II/LC3I, Beclin1, p62, p-IGF-1 R, p-PI3k, p-Akt and FOXO3 expression. Data were expressed as mean \pm SD. N = 3. * $P < 0.05$, ** $P < 0.01$, *** $P < 0.001$ (vs. NC group).

tissues and adjacent non-tumor tissues was monitored by RT-PCR, which substantiated that the IGF1 level in OS tissues was higher versus non-tumor tissues adjacent to tumor ($P < 0.05$, Figure 5(e)). Furthermore, WB illustrated that the IGF1 expression in OS cell lines was generally higher than that in hFOB 1.19 ($P < 0.05$, Figure 5(f)). Meanwhile, RT-PCR testified that transfection of agomir-miR-29a-3p in OS cell lines resulted in lower expression of IGF1 versus the NC group ($P < 0.05$, Figure 5(g)). These outcomes hinted that miR-29a-3p targeted IGF1 and was an underlying therapeutic target for OS, while IGF1 was up-regulated in OS.

3.6 IGF1 enhanced OS cell proliferation, colony formation, migration and invasion, and abated apoptosis and autophagy

The above studies imply that miR-29a-3p targets IGF1, but it is poorly understood about the role of

IGF1 in OS. Hence, we treated MG-63 cells with IGF1 (100 ng/mL), the IGF-1 R inhibitor Linsitinib (OSI-906,75 nM), and the PI3K inhibitor SF2523 (34 nM) for confirming IGF1-mediated mechanism. OS cell proliferation, colony formation, apoptosis, migration and invasion were monitored by the MTT assay, colony formation experiment, western blot and transwell assay. Interestingly, IGF1 treatment enhanced OS cell proliferation, migration, invasion, colony formation and EMT and abated apoptosis. Inhibition of IGF-1 R or PI3K led to the depression of OS cell proliferation, migration, invasion, and EMT and increment of apoptosis ($P < 0.05$, Figure 6(a-f)). Further, WB gauged the expression of LC3II/LC3I, Beclin1, up-regulated p62, activated IGF-1 R, PI3k and Akt phosphorylation, and down-regulated FOXO3. In contrast, attenuation of IGF-1 R raised LC3II/LC3I and Beclin1 expression, down-regulated

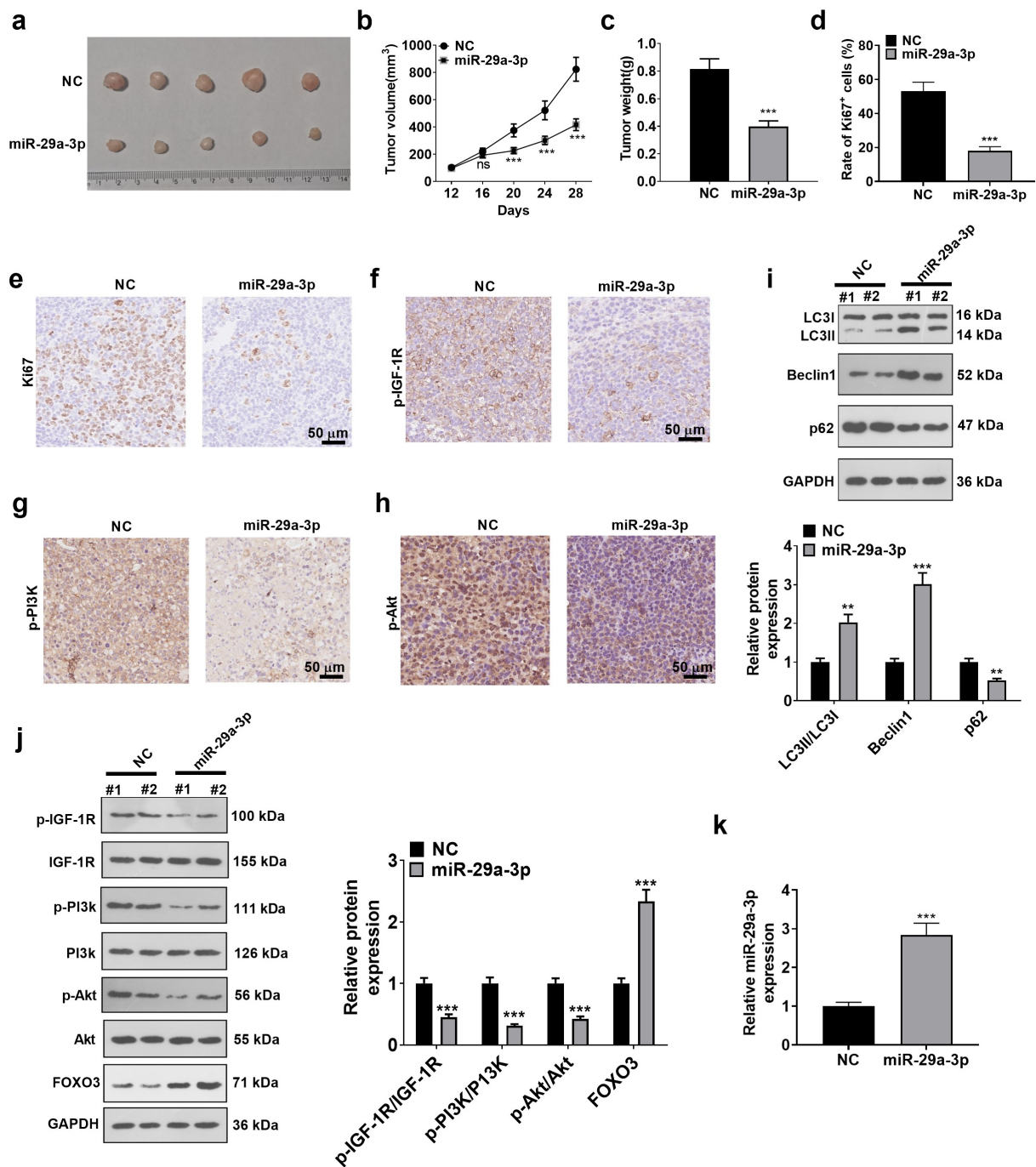


Figure 4. miR-29a-3p curbed OS growth and facilitated autophagy *in vivo*. MG-63 cells transfected with miR-29a-3p agomir and agomir-NC were subcutaneously injected in nude mice. A: Diagram of a subcutaneously excised tumor. B: The tumor volume was determined from the 12th day after the tumor formation experiment and then gauged every 4 days. C: The mice were sacrificed on the 28th day, and the tumor was cut out and weighed. D-G: IHC checked the expression of Ki67 (Figure 4d-e), p-IGF-1 R (figure 4f), p-PI3K (Figure 4g) and p-AKT (Figure 4h) in tumor tissues. Scale bar = 50 μm. I and J: WB was employed to monitor the expression of LC3II/LC3I, Beclin1, p62, p-IGF-1 R, p-PI3k, p-Akt and FOXO3 in tissues. K: The miR-29a-3p level in tumor tissues was estimated by RT-PCR. Data were expressed as mean ± SD. n = 5. nsP > 0.05, *P < 0.05, **P < 0.01, ***P < 0.001 (vs. NC group).

p62, repressed phosphorylation of IGF-1 R, PI3k and Akt, and up-regulated FOXO3. More notably, PI3K inhibition stimulated the autophagic pathway,

dampened the phosphorylation of PI3k and Akt, and up-regulated FOXO3, but it had no significant impact on p-IGF-1 R expression ($P < 0.05$, Figure 6

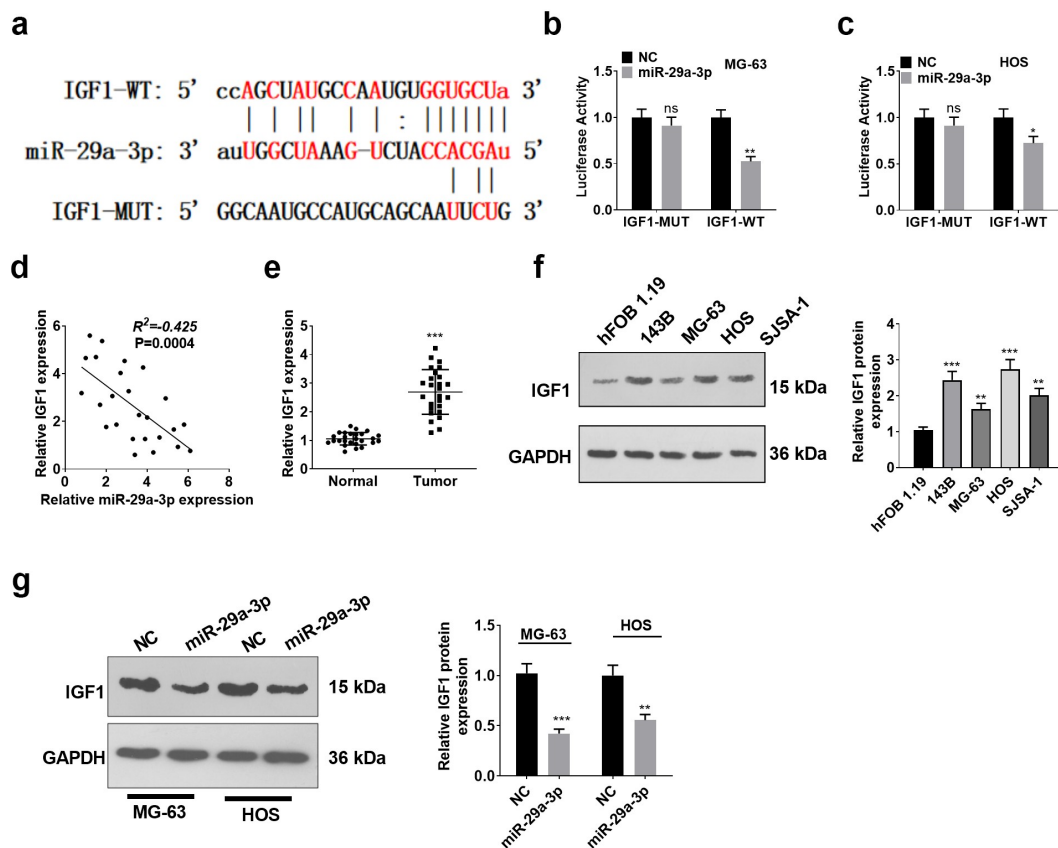


Figure 5. miR-29a-3p targeted IGF1. A: The miR-29a-3p downstream targets were queried by Starbase (<http://starbase.sysu.edu.cn/>). B-C: The dual-luciferase reporter assay was employed to test the expression of IGF1-MUT and IGF1-WT, ns $P > 0.05$, * $P < 0.05$; ** $P < 0.01$ (vs. NC group); D: Pearson correlation analysis was implemented to verify the relationship between miR-29a-3p and IGF1 in OS tissues; E: The IGF1 profile in OS and adjacent normal tissues was monitored by RT-PCR, *** $P < 0.001$; F-G: WB tested the IGF1 expression. ** $P < 0.01$; *** $P < 0.001$ (vs. hFOB 1.19 group).

(g, h)). These data substantiated that IGF1 exacerbated the malignant behaviors of OS cells, hindered autophagy, and activated the IGF-1 R/PI3k/Akt axis.

3.7 IGF1 weakened the tumor-suppressive effect of miR-29a-3p

We conducted a compensation experiment to verify the effect of IGF1 on miR-29a-3p's tumor-suppressive effects. Briefly, IGF1 (100 ng/ml) was administered into MG-63 cells with agomir-miR-29a-3p transfection, and RT-PCR was conducted to measure the miR-29a-3p level. It was found that IGF1 didn't significantly alter miR-29a-3p level ($P > 0.05$ vs. miR-29a-3p group, Figure 7(a)). Then, the MTT assay, colony formation experiment, western blot and transwell assay were adopted to verify MG-63 cell proliferation, colony, apoptosis, migration and invasion. Interestingly, by contrast with the miR-29a-3p group, IGF1

increased OS cell proliferation, migration, invasion and colonies ($P < 0.5$, Figure 7(b-e)). The Western blot results showed that compared with miR-29a-3p group, IGF1 treatment reduced Bax, Bad, LC3II/LC3I, Beclin1, E-cadherin, FOXO3, whereas promoted Bcl2, N-cadherin, Vimentin, p62, p-IGF-1 R, p-PI3k and p-Akt expression ($P < 0.5$, Figure 7(h, i)). Hence, IGF1 partially eliminated the tumor-suppressive effect of miR-29a-3p on OS.

4 Discussion

OS is the most commonly seen malignant bone tumor in young people. For decades, OS patients' five-year survival rate has been stagnant at around 70% [24]. In this setting, the rising incidence rate and the declining overall cure rate are insidious. In particular, the five-year survival rate of metastatic OS can be reduced to 20%-30% [25]. As reported, noncoding RNAs subserve the diagnosis,

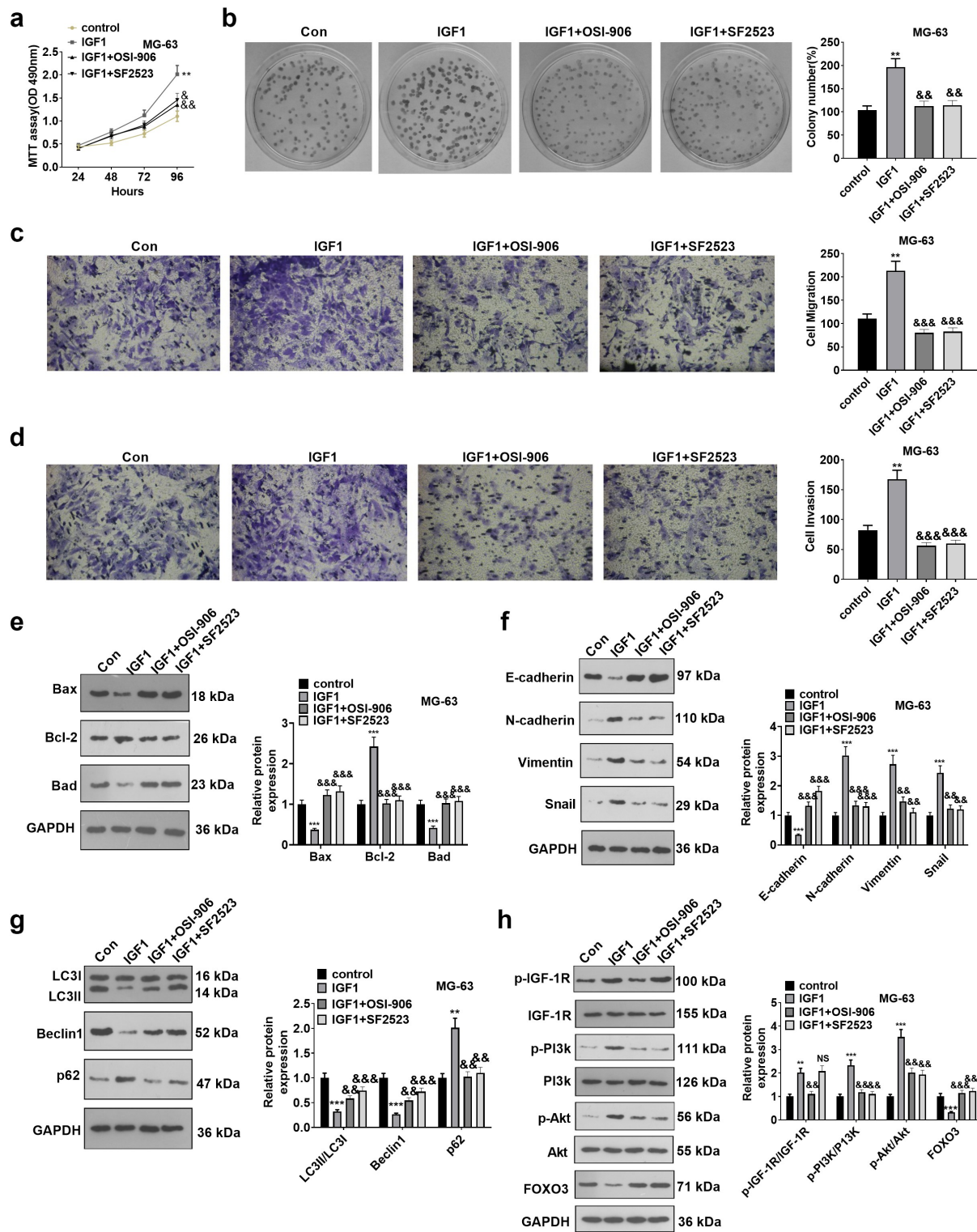


Figure 6. IGF1 enhanced OS proliferation, colony formation, migration and invasion, and abated apoptosis and autophagy. We treated MG-63 cells with IGF1 (100 ng/mL), the IGF-1 R inhibitor Linsitinib (OSI-906,75 nM), and the PI3K inhibitor SF2523 (34 nM) for 24 hours, respectively. A: MTT assay was employed to testify cell proliferation. B: The colony formation experiment was adopted to count cell colonies. C-D: Transwell assay was implemented to verify cell migration and invasion. E: WB checked the expression of Bax, Bcl-2 and Bad in cells. F: WB tested the profiles of E-cadherin, N-cadherin, Vimentin, and Snail in cells. G and H: WB was conducted to examine the expression of LC3II/LC3I, Beclin1, p62, p-IGF-1 R, p-PI3K, p-Akt and FOXO3 in tissues. Data were expressed as mean \pm SD. N = 3. * P < 0.05; ** P < 0.01; *** P < 0.001 (vs. control group).

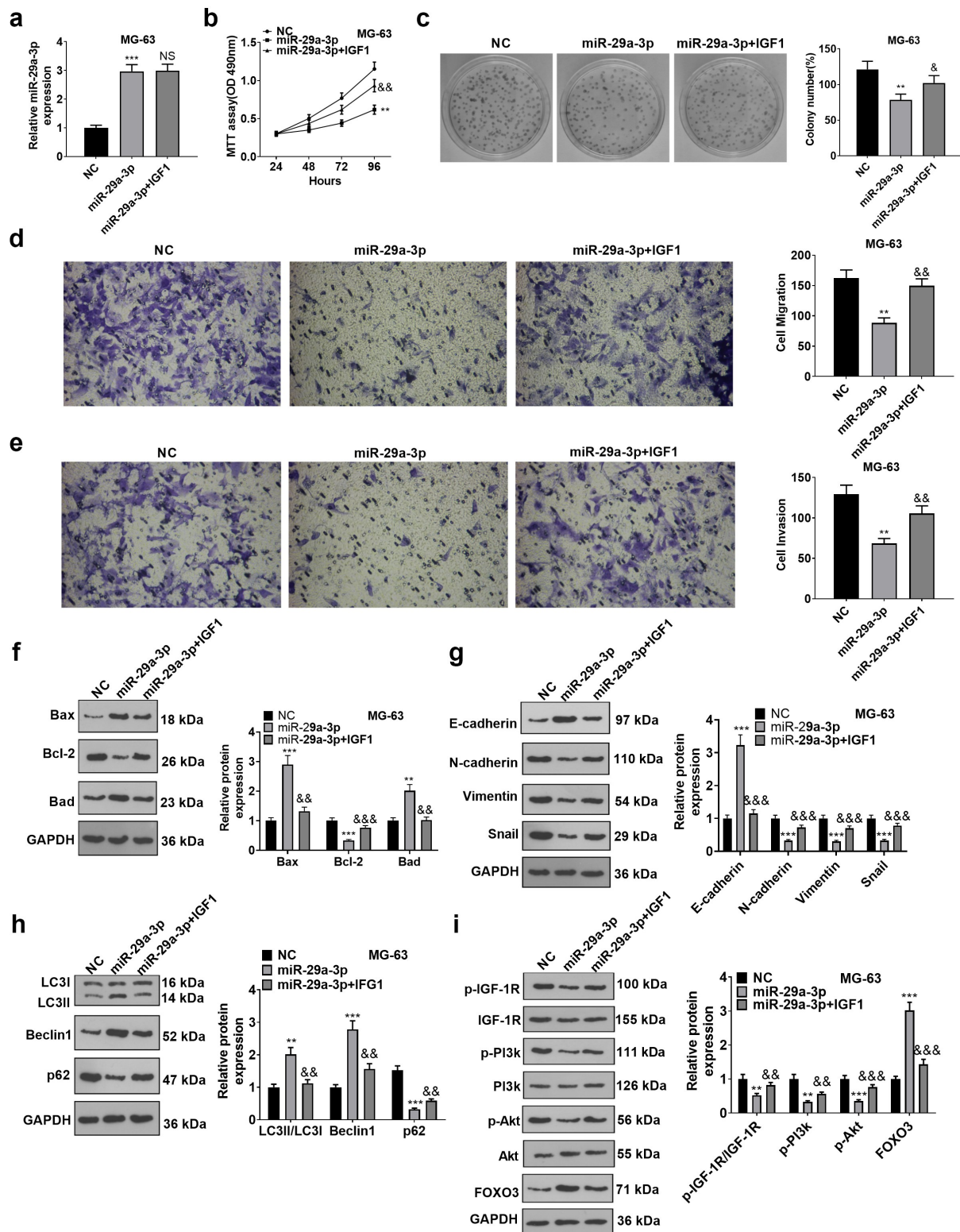


Figure 7. Overexpressing IGF1 suppressed the anti-tumor effects of miR-29a-3p. MG-63 cells were transfected with miR-29a-3p agomir and/or treated with IGF1 (100 ng/ml) for 24 hours. A: RT-PCR was conducted to test the miR-29a-3p profile. B: The MTT assay was implemented to monitor cell proliferation; C: The number of cell colonies was counted by the colony formation test. D-E. Transwell assay was implemented to verify cell migration and invasion. F: The protein levels of Bax, Bcl-2 and Bad were compared by WB. G: WB assayed E-cadherin, N-cadherin, Vimentin, and Snail expression. H and I: WB was done to monitor the expression of LC3II/LC3I, Beclin1, p62, p-IGF-1 R, p-PI3k, p-Akt and FOXO3 in tissues. Data were expressed as mean \pm SD. N = 3. * P < 0.05; ** P < 0.01; *** P < 0.001 (vs. NC group); # P < 0.05; ## P < 0.01; ### P < 0.001 (vs. miR-29a-3p group).

treatment, and prognosis of OS [26–28]. Here, we study the specific mechanism by which miR-29a-3p targets IGF1 to regulate autophagy and influence the progress of OS. We observed that overexpressing miR-29a-3p retarded the proliferation, migration and invasion of MG63 and U2OS cells and induced apoptosis. At the same time, we concluded that miR-29a-3p exerted tumor-suppressive effects by targeting IGF1 to repress the PI3K/Akt axis and thereby up-regulating FOXO3 (Figure 8).

Autophagy is a highly conservative metabolic breakdown mechanism first proposed by Christian de Duve in 1963. Autophagy has been increasingly identified as a possible target for treating malignancies in the last few years [29]. For instance, Zhang et al. held that DEAD-box protein 5 (DDX5) activates autophagy through the p62/SQSTM1 axis, thereby dampening the occurrence and development of hepatocellular carcinoma [30]. A similar autophagic effect is also observed in OS. For example, Liu et al. proved that Apatinib induces OS autophagy and promotes apoptosis by inhibiting VEGFR2, STAT3 and BCL-2, thus inhibiting OS [31]. Also, estrogen receptor β (ER β) exerts an anti-proliferative role in OS by inducing autophagy [32]. Besides, STF cDNA 3 (TSSC3) strengthens autophagy by attenuating the PI3k/Akt/mTOR axis to slow the occurrence and

metastasis of OS [33]. Thus, activating autophagy is a new target for OS therapy. This study reveals that autophagy is activated by miR-29a-3p in OS, thereby contributing to tumor repression.

MiRNAs bind to the mRNA 3'-UTR of their target genes, thereby silencing the target gene's mRNAs. Recent studies have confirmed that miRNAs have great potential in cancer diagnosis, treatment and prognosis [34]. Also, the anti-tumor characteristics of miRNAs are present in OS. For instance, miR-223-3p is down-regulated in OS, which dampens tumor metastasis and progression by targeting Cadherin-6 [35]. As another example, overexpressing miR-139-5p attenuates cell proliferation, migration and invasion, and inhibits OS development by targeting DNA methyltransferase-1 [36]. Besides, miR-761 inactivates the PI3k/Akt pathway through fibroblast growth factor receptor 1 and exerts the inhibitory effect in OS [37]. Moreover, miR-29a-3p is absent in multiple cancers and is considered a tumor suppressor. Meanwhile, miR-29a-3p is reported to negatively regulate myeloid cell leukemia sequence 1, which is a possible target for the diagnosis and treatment of acute myeloid leukemia [38]. Another study revealed that miR-29a-3p targets Prominin 1 to inhibit laryngeal cancer cell proliferation [39]. Furthermore, Ma et al. claimed that overexpressing miR-29a-3p inhibits NF- κ B through OTUB2, thereby attenuating cell proliferation, invasion and growth in papillary thyroid cancer [40]. However, there are few reports about the function of miR-29a-3p in OS. Hence, we speculated that miR-29a-3p also restrained OS. Fortunately, our experiments testified that the expression of miR-29a-3p is absent in OS, and the transfection of agomir miR-29a-3p abated cell proliferation, migration, invasion and colony formation and facilitated apoptosis both *in vivo* and *in vitro*, resembling the above research and confirming our predictions.

The activation of the IGF family accelerates the development and metastasis of cancer and causes pathological growth and differentiation [41]. For instance, Lei et al. found that IGF1 expedites the growth and metastasis of hepatocellular carcinoma by dampening the degradation of Cathepsin B [42]. Also, Dang et al. reported that miR-3941 targets and negatively modulates IGF1 and refrains

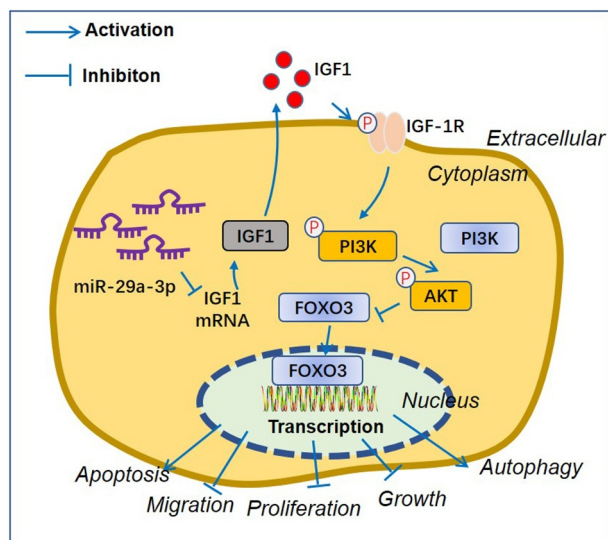


Figure 8. The Schematic diagram. MiR-29a-3p is downregulated in OS cells. miR-29a-3p targets IGF1 and inhibits its expression. IGF1 activates IGF-1 R/PI3K/AKT/FOXO3 pathway and induces enhanced migration, invasion, proliferation and growth of OS cells.

cell proliferation, migration and invasion of breast cancer [43]. It is worth noting that the aberrant expression of IGF1 is strongly linked to some bone diseases [44,45]. On this basis, we are very curious about the impact of IGF1 on OS. Literature studies have found that IGF1, an important target of miR-29, enhances OS angiogenesis [46]. Besides, Armakolas et al. held that the IGF1 level is implicated in the poor prognosis of OS [47]. Moreover, miR-26a targets and inhibits the IGF1 expression, thereby exerting anti-tumor effects in OS [48]. Similarly, our study discovered that overexpression of IGF1, an important downstream target of miR-29a-3p, not only aggravated the malignant biological behaviors of OS, but also counteracted the tumor-suppressive function of miR-29a-3p.

The PI3k/Akt signal is involved in various biological processes and is often abnormally activated in cancer. Its transcriptional activation is implicated in cell growth and proliferation and contributes to tumor progression by regulating epigenetic genes [49]. As an example, Tang et al. have corroborated that miR-133a-3p avoids bone metastasis of prostate cancer by inhibiting the PI3k/Akt axis [50]. Additionally, Chen et al. showed that miR-191-5p targets EGR1 to trigger the PI3k/Akt pathway and expedite OS evolution [51]. Other studies have shown that miR-939-5p inactivates the PI3k/Akt axis by regulating IGF1 R, thereby suppressing OS [52]. On the other hand, the inhibitory effect of FOXO3 in malignant tumors has been well-established [53,54]. Meanwhile, FOXO3 is an autophagy degradation substrate, which corrects autophagy inhibition by activating autophagy-related genes [55]. More importantly, Mitoxantrone induces OS apoptosis and inhibits cell proliferation through the Akt/FOXO3 axis [56]. Here, we found through experiments that miR-29a-3p promotes autophagy, inactivates the PI3k/Akt axis, and increases the FOXO3 level. In parallel, IGF1 is reversely modulated by miR-29a-3p, and overexpressing IGF1 attenuates autophagy, activates the PI3k/Akt signaling pathway, and dampens the FOXO3 level.

Collectively, miR-29a-3p is down-regulated in OS, and it obviously dampens the malignant biological behaviors of OS and promotes autophagy by regulating the PI3k/Akt/FOXO3 axis. Meanwhile, IGF1 is a vital downstream target of miR-29a-3p. miR-29a-

3p targets IGF1 to control the PI3k/Akt/FOXO3 axis, activates autophagy, and inhibits OS progression. This study provides the impetus for formulating a new treatment strategy for OS, while it needs further in-depth research for clinical application.

Authors contribution

Conceived and designed the experiments: Qi Song, Li Xu, Hongkun Chen;

Performed the experiments: Qi Song, Li Xu, Yongyuan Han, Yongyuan Han;

Statistical analysis: Qi Song, Li Xu, Yongyuan Han;

Wrote the paper: Qi Song, Hongkun Chen, Anyuan Cheng.

All authors read and approved the final manuscript.

Disclosure statement

No potential conflict of interest was reported by the author(s).

Funding

This research did not receive any specific grant from funding agencies in the public, commercial, or not-for-profit sectors.

Ethics statement

Our study was approved by the Ethics Review Board of Wuhan No 1 Hospital.

Data availability

The data sets used and analyzed during the current study are available from the corresponding author on reasonable request.

References

- [1] Luetke A, Meyers PA, Lewis I, et al. Osteosarcoma treatment - where do we stand? A state of the art review. *Cancer Treat Rev.* 2014;40(4):523–532.
- [2] Meyers PA, Heller G, Healey JH, et al. Osteogenic sarcoma with clinically detectable metastasis at initial presentation. *J Clin Oncol.* 1993;11(3):449–453.
- [3] Levine B, Kroemer G. Biological functions of autophagy genes: a disease perspective. *Cell.* 2019;176(1–2):11–42.
- [4] Onorati AV, Dyczynski M, Ojha R, et al. Targeting autophagy in cancer. *Cancer.* 2018;124(16):3307–3318.
- [5] Camuzard O, Santucci-Darmanin S, Carle GF, et al. Role of autophagy in osteosarcoma. *J Bone Oncol.* 2019;16:100235.

- [6] Dong SW, Xiao YB, Ma X, et al. miR-193b increases the chemosensitivity of osteosarcoma cells by promoting FEN1-mediated autophagy. *Onco Targets Ther.* **2019**;12:10089–10098.
- [7] Svoronos AA, Engelman DM, Slack FJ. OncomiR or tumor suppressor? The duplicity of MicroRNAs in cancer. *Cancer Res.* **2016**;76(13):3666–3670.
- [8] Liu F, Wang XD. miR-150-5p represses TP53 tumor suppressor gene to promote proliferation of colon adenocarcinoma. *Sci Rep.* **2019**;9(1):6740.
- [9] Dai FQ, Li CR, Fan XQ, et al. miR-150-5p inhibits non-small-cell lung cancer metastasis and recurrence by targeting HMGA2 and β -catenin signaling. *Mol Ther Nucleic Acids.* **2019**;16:675–685.
- [10] Liu Q, Wang Z, Zhou X, et al. miR-342-5p inhibits osteosarcoma cell growth, migration, invasion, and sensitivity to Doxorubicin through targeting Wnt7b. *Cell Cycle.* **2019** Dec;18(23):3325–3336. Epub 2019 Oct 10.
- [11] Liu K, Huang J, Ni J, et al. MALAT1 promotes osteosarcoma development by regulation of HMGB1 via miR-142-3p and miR-129-5p. *Cell Cycle.* **2017** Mar 19;16(6):578–587. Epub 2017 Feb 10.
- [12] Wang L, Liu Y. Long noncoding RNA RHPN1-AS1 exerts pro-oncogenic actions in osteosarcoma by functioning as a molecular sponge of miR-506 to positively regulate SNAI2 expression. *Cell Cycle.* **2020** Jun;19(12):1517–1529. Epub 2020 May 13.
- [13] Wang F, Zhao QH, Liu JZ, et al. MiRNA-188-5p alleviates the progression of osteosarcoma via target degrading CCNT2. *Eur Rev Med Pharmacol Sci.* **2020** Jan;24(1):29–35.
- [14] Zheng ZL, Cui HT, Wang Y, et al. Downregulation of RPS15A by miR-29a-3p attenuates cell proliferation in colorectal carcinoma. *Biosci Biotechnol Biochem.* **2019**;83(11):2057–2064.
- [15] Wang X, Liu SS, Cao L, et al. miR-29a-3p suppresses cell proliferation and migration by downregulating IGF1R in hepatocellular carcinoma. *Oncotarget.* **2017**;8(49):86592–86603.
- [16] Chao S, Wang WC, Wang CC. IGF-1-induced MMP-11 expression promotes the proliferation and invasion of gastric cancer cells through the JAK1/STAT3 signaling pathway. *Oncol Lett.* **2018**;15(5):7000–7006.
- [17] Li YS, Liu Q, He HB, et al. The possible role of insulin-like growth factor-1 in osteosarcoma. *Curr Probl Cancer.* **2019**;43(3):228–235.
- [18] Wang J, Zhang Y, Dou ZX, et al. Knockdown of STIL suppresses the progression of gastric cancer by downregulating the IGF-1/PI3k/AKT pathway. *J Cell Mol Med.* **2019**;23(8):5566–5575.
- [19] Chen Y, Huang WD, Sun W, et al. LncRNA MALAT1 promotes cancer metastasis in osteosarcoma via activation of the PI3k-Akt signaling pathway. *Cell Physiol Biochem.* **2018**;51(3):1313–1326.
- [20] Brunet A, Bonni A, Zigmond MJ, et al. Akt promotes cell survival by phosphorylating and inhibiting a forkhead transcription factor. *Cell.* **1999**;96(6):857–868.
- [21] Rupp M, Hagenbuchner J, Rass B, et al. FOXO3-mediated chemo-protection in high-stage neuroblastoma depends on wild-type TP53 and SESN3. *Oncogene.* **2017**;36(44):6190–6203.
- [22] Zhou YF, Li SX, Li JT, et al. Effect of microRNA-135a on cell proliferation, migration, invasion, apoptosis and tumor angiogenesis through the IGF-1/PI3k/Akt signaling pathway in non-small cell lung cancer. *Cell Physiol Biochem.* **2017**;42(4):1431–1446.
- [23] Wang Y, Zhang R, Cheng G, et al. Long noncoding RNA HOXA-AS2 promotes migration and invasion by acting as a ceRNA of miR-520c-3p in osteosarcoma cells. *Cell Cycle.* **2018**;17(13):1637–1648.
- [24] Corre I, Verrecchia F, Crenn V, et al. The osteosarcoma microenvironment: a complex but targetable ecosystem. *Cells.* **2020**;9(4):976.
- [25] Ferguson JL, Turner SP. Bone cancer: diagnosis and treatment principles. *Am Fam Physician.* **2018**;98(4):205–213.
- [26] Wang CY, Ren M, Zhao X, et al. Emerging roles of circular RNAs in osteosarcoma. *Med Sci Monit.* **2018**;24:7043–7050.
- [27] Li ZH, Dou PC, Liu T, et al. Application of long noncoding RNAs in osteosarcoma: biomarkers and therapeutic targets. *Cell Physiol Biochem.* **2017**;42(4):1407–1419.
- [28] Wang JC, Liu SZ, Shi JY, et al. The role of miRNA in the diagnosis, prognosis, and treatment of osteosarcoma. *Cancer Biother Radiopharm.* **2019**;34(10):605–613.
- [29] Kocaturk NM, Akkoc Y, Kig C, et al. Autophagy as a molecular target for cancer treatment. *Eur J Pharm Sci.* **2019**;134:116–137.
- [30] Zhang H, Zhang YQ, Zhu XY, et al. DEAD box protein 5 inhibits liver tumorigenesis by stimulating autophagy via interaction with p62/SQSTM1. *Hepatology.* **2019**;69(3):1046–1063.
- [31] Liu KS, Ren TT, Huang Y, et al. Apatinib promotes autophagy and apoptosis through VEGFR2/STAT3/BCL-2 signaling in osteosarcoma. *Cell Death Dis.* **2017**;8(8):e3015.
- [32] Yang ZM, Yang MF, Yu W, et al. Molecular mechanisms of estrogen receptor β -induced apoptosis and autophagy in tumors: implication for treating osteosarcoma. *J Int Med Res.* **2019**;47(10):4644–4655.
- [33] Zhao GS, Tang XF, Lv YF, et al. TSSC3 promotes autophagy via inactivating the Src-mediated PI3k/Akt/mTOR pathway to suppress tumorigenesis and metastasis in osteosarcoma, and predicts a favorable prognosis. *J Exp Clin Cancer Res.* **2018**;37(1):188.
- [34] Rupaimoole R, Slack FJ. MicroRNA therapeutics: towards a new era for the management of cancer and other diseases. *Nat Rev Drug Discov.* **2017**;16(3):203–222.

- [35] Ji QB, Xu XJ, Song Q, et al. miR-223-3p inhibits human osteosarcoma metastasis and progression by directly targeting CDH6. *Mol Ther.* **2018**;26(5):1299–1312.
- [36] Shi YK, Guo YH. MiR-139-5p suppresses osteosarcoma cell growth and invasion through regulating DNMT1. *Biochem Biophys Res Commun.* **2018**;503(2):459–466.
- [37] Lv ZZ, Ma JM, Wang JC, et al. MicroRNA-761 targets FGFR1 to suppress the malignancy of osteosarcoma by deactivating PI3k/Akt pathway. *Onco Targets Ther.* **2019**;12:8501–8513.
- [38] Gado MM, Mousa NO, Badawy MA, et al. Assessment of the diagnostic potential of miR-29a-3p and miR-92a-3p as circulatory biomarkers in acute myeloid Leukemia. *Asian Pac J Cancer Prev.* **2019**;20(12):3625–3633.
- [39] Su JL, Lu EY, Lu LJ, et al. miR-29a-3p suppresses cell proliferation in laryngocarcinoma by targeting prominin 1. *FEBS Open Bio.* **2017**;7(5):645–651.
- [40] Ma YF, Sun Y. miR-29a-3p inhibits growth, proliferation, and invasion of papillary thyroid carcinoma by suppressing NF- κ B signaling via direct targeting of OTUB2. *Cancer Manag Res.* **2018**;11:13–23.
- [41] Cevenini A, Orrù S, Mancini A, et al. Molecular signatures of the insulin-like growth factor 1-mediated epithelial-mesenchymal transition in breast, lung and gastric cancers. *Int J Mol Sci.* **2018**;19(8):2411.
- [42] Lei T, Ling X. IGF-1 promotes the growth and metastasis of hepatocellular carcinoma via the inhibition of proteasome-mediated cathepsin B degradation. *World J Gastroenterol.* **2015**;21(35):10137–10149.
- [43] Dang XG, Li XQ, Wang L, et al. MicroRNA-3941 targets IGF-1 to regulate cell proliferation and migration of breast cancer cells. *Int J Clin Exp Pathol.* **2017**;10(7):7650–7660.
- [44] Yakar S, Werner H, Rosen CJ. Insulin-like growth factors: actions on the skeleton. *J Mol Endocrinol.* **2018**;61(1):T115–T137.
- [45] Chen SX, Du ZP, Wu BL, et al. STAT1, IGF1, RAC1, and MDM2 are associated with recurrence of giant cell tumor of bone. *J Immunol Res.* **2018**;2018:4564328.
- [46] Gao SM, Cheng C, Chen HW, et al. IGF1 3'UTR Functions as a ceRNA in promoting angiogenesis by Sponging miR-29 family in osteosarcoma. *J Mol Histol.* **2016**;47(2):135–143.
- [47] Mao JS, Zhuang GY, Chen ZK. Genetic polymorphisms of insulin-like growth factor 1 are associated with osteosarcoma risk and prognosis. *Med Sci Monit.* **2017**;23:5892–5898.
- [48] Tan XY, Fan SC, Wen W, et al. MicroRNA-26a inhibits osteosarcoma cell proliferation by targeting IGF-1. *Bone Res.* **2015**;3(1):15033.
- [49] Spangle JM, Roberts TM, Zhao JJ. The emerging role of PI3k/AKT-mediated epigenetic regulation in cancer. *Biochim Biophys Acta Rev Cancer.* **2017**;1868(1):123–131.
- [50] Tang YB, Pan JC, Huang S, et al. Downregulation of miR-133a-3p promotes prostate cancer bone metastasis via activating PI3k/AKT signaling. *J Exp Clin Cancer Res.* **2018**;37(1):160.
- [51] Chen Y, Zheng ZY, Yang JZ, et al. MicroRNA-191-5p promotes the development of osteosarcoma via targeting EGR1 and activating the PI3k/AKT signaling pathway. *Eur Rev Med Pharmacol Sci.* **2019**;23(9):3611–3620.
- [52] Zhao XW, Li J, Yu DP. MicroRNA-939-5p directly targets IGF-1R to inhibit the aggressive phenotypes of osteosarcoma through deactivating the PI3k/Akt pathway. *Int J Mol Med.* **2019**;44(5):1833–1843.
- [53] Zhu DD, Yuan DL, Guo RF, et al. Overexpression of miR-148a inhibits viability and invasion of ovarian cancer OVCAR3 cells by targeting FOXO3. *Oncol Lett.* **2019**;18(1):402–410.
- [54] Zhang HY, Zhang Z, Wang SR, et al. The mechanisms involved in mir-9 regulated apoptosis in cervical cancer by targeting FOXO3. *Biomed Pharmacother.* **2018**;102:626–632.
- [55] Fitzwalter BE, Thorburn A. FOXO3 links autophagy to apoptosis. *Autophagy.* **2018**;14(8):1467–1468.
- [56] Park SH, Lee JS, Kang MA, et al. Mitoxantrone induces apoptosis in osteosarcoma cells through regulation of the Akt/FOXO3 pathway. *Oncol Lett.* **2018**;15(6):9687–9696.